

# СЕНСОРИ ФІЗИЧНИХ ВЕЛИЧИН PHYSICAL SENSORS

PACS: 72.80.Le

## DC AND AC MEASUREMENTS ON ITO/NIPC/METAL CELLS IN HUMID ENVIRONMENT

Z. Yu. Hotra<sup>1</sup>, G. L. Pakhomov<sup>2</sup>, N. V. Kostiv<sup>1</sup>, P. Y. Stakhira<sup>1</sup>, I. I. Hryhorchak<sup>3</sup>, V. V. Cherpak<sup>1</sup>, D. Yu. Volyniuk<sup>1</sup>

<sup>1</sup> Electronic device department, Lviv Polytechnic National University, S. Bandera, 12, Lviv, 79013 Ukraine

<sup>2</sup> Institute for Physics of Microstructures of the Russian Academy of Sciences, GSP-105, Nizhny Novgorod, 603950, Russian Federation

<sup>3</sup> Department of engineering, materials science and applied physics, Lviv Polytechnic National University, S. Bandera, 12, Lviv, 79013 Ukraine

e-mail: zhotra@polynet.lviv.ua

e-mail: pakhomov@ipm.sci-nnov.ru

e-mail: natalyakostiv@yahoo.com

e-mail: stakhira@polynet.lviv.ua

e-mail: vlcherpak@yahoo.com

e-mail: ivangr@rambler.ru

e-mail: dvolynyuk@rambler.ru

## DC AND AC MEASUREMENTS ON ITO/NIPC/METAL CELLS IN HUMID ENVIRONMENT

Z. Yu. Hotra, G. L. Pakhomov, N. V. Kostiv, P. Y. Stakhira, I. I. Hryhorchak, V. V. Cherpak, D. Yu. Volyniuk

**Abstract.** Current density-vs-voltage characteristics and frequency dependences of impedance were analyzed for sandwich cells ITO/NiPc/Metal, where ITO is a transparent conducting double indium-tin oxide, NiPc is a thermally evaporated nickel phthalocyanine thin film, and Metal is aluminum or indium top electrode. After testing in dry air, these cells were exposed to saturated water vapors, or mixed water/ammonia vapors with different pressures. Comparative analysis of the data taken from DC and AC measurements in the dark was carried out. Contributions of the NiPc film bulk and the NiPc/Metal interfacial region to conducting properties of the cells were elucidated. Impedance of the cells in various environments was interpreted using equivalent circuits, and the time scales for relaxation processes in NiPc films were thus estimated.

**Keywords:** nickel phthalocyanine; ammonia vapors; AC conductivity measurements; DC conductivity measurements

## ДОСЛІДЖЕННЯ ЕЛЕКТРОПРОВІДНОСТІ СТРУКТУР ИТО/NIPC/МЕТАЛЕВИЙ ЕЛЕКТРОД В РІЗНИХ ГАЗОВИХ СЕРЕДОВИЩАХ

3. Ю. Готра, Г. Л. Пахомов, Н. В. Костів, П. Й. Стакіра, І. І. Григорчак, В. В. Черпак,  
Д. Ю. Волинюк

**Анотація.** Досліджені вольт-амперні та імпедансні характеристики структур ИТО/NiPc/металевий електрод. Структури сформовані методом термовакуумного напилення почерговим нанесенням на скляні підкладки з оптично-прозорим електродом ИТО плівок органічного напівпровідника фталоціаніну нікелю (NiPc) та металевих електродів алюмінію або індію. Дослідження структур проведено в середовищах повітря, наасиченої водяної пари та наасичених парів водних розчинів аміаку різного парціального тиску. Проведений порівняльний аналіз постійних та змінних темнових струмів структур. Встановлені електропровідні характеристики досліджуваних структур в залежності від властивостей плівки NiPc та інтерфейсу NiPc/металевий електрод під впливом різних газових середовищах. Оцінені процеси релаксації в плівці NiPc на основі моделювання еквівалентних схем структур відповідно до імпедансних досліджень.

**Ключові слова:** фталоціанін нікелю, наасичена пара аміаку, дослідження змінного струму, дослідження постійного струму

## ИССЛЕДОВАНИЯ ЭЛЕКТРОПРОВОДИМОСТИ СТРУКТУР ИТО/NIPC/ МЕТАЛЛИЧЕСКИЙ ЭЛЕКТРОД В РАЗНЫХ ГАЗОВЫХ СРЕДАХ

3. Ю. Готра, Г. Л. Пахомов, Н. В. Костів, П. Й. Стакіра, І. І. Григорчак,  
В. В. Черпак, Д. Ю. Волинюк

**Аннотация.** Исследовано вольтамперные и импедансные характеристики структур ИТО/NiPc/металлический электрод. Структуры сформированы методом термовакуумного испарения последовательным нанесением на стеклянные подложки с оптически прозрачным электродом ИТО плёнок органического полупроводника фталоцианина никеля (NiPc) и металлических электродов алюминия или индия. Структуры исследовались в атмосферах воздуха, насыщенной водяной пары и насыщенных водных растворах аммиака разных парциальных давлений. Проведено сравнительный анализ постоянных и переменных темновых токов структур. Установлено электропроводные характеристики исследованных структур в зависимости от свойств плёнки NiPc и интерфейса NiPc/металлический электрод под воздействием разных газовых сред. Оценены процессы релаксации в плёнке NiPc на основании моделирования эквивалентных схем структур в соответствии к импедансным исследованиям.

**Ключевые слова:** фталоцианин никеля, насыщенная пара аммиака, исследования переменного тока, исследования постоянного тока

### 1. Introduction

The sandwich structures containing a thin film of semiconducting metal phthalocyanine complex and a low work function metallic electrode are the simplest example of organic Schottky-type photovoltaic cells. Although such type of cells demonstrates fairly low power conversion efficiencies, it may potentially be interesting in some photovoltaic applications [1-3] (due to, e.g., a higher open circuit voltage  $V_{oc}$  [4] than that commonly reported for heterojunction based cells) or in chemical sensors [5-8].

Diode properties and photoassisted conductivity in such cells are simultaneously governed by several factors like morphology of molecular layer, or its ability to absorb various non-resident admixtures coming from environment. These are oxygen or water molecules, if the cells operate in non-inert atmospheres [7,9-11].

Thickness of molecular layer typically does not exceed few hundreds nanometers, while boundaries are fuzzy and effective electrode area is in order of square millimeters. Therefore, the bulk processes are often obscured by a large con-

tribution of interfacial effects [1,3,12]. Interfaces, mostly, but not exclusively [9,13], with reactive metals, are of paramount importance for efficient charge injection. There is an uncertainty in the actual composition of the interface, since i) reactions between hot depositing metal atoms and molecular surface are possible [14] and ii) top deposited metal atoms (or reaction products) diffuse into the film bulk. The latter process often leads to short-circuits when measuring vertical conductivity in the cells.

On the other hand, absorbed species (oxygen or water molecules) may freely diffuse inside the phthalocyanine layer towards the electrodes [7] and give rise to redox and electrochemical processes on the boundaries [9,10,12,15]. So, ionic conduction passes appear in the cells, complementary to measured electronic current. This explains appearance of nonzero current at zero voltage during conductivity measurements in the dark and/or non-reversible drift of cell's parameters. Murata et al. concluded that photocurrent in ITO/porphyrin/Al cells originates from irradiation-assisted oxidation (photocorrosion) of aluminum contact [2,16]. In our earlier works [12,15,17] we observed generation of output electrical power in the dark when the cells incorporating a metal phthalocyanine/aluminum barrier where exposed to chemically active environments. It was assigned to electrochemical reactions involving metallic cathode and its oxide components.

All the above mentioned is derived from direct current (DC) measurements. However, more reliable information can be inferred from the time (frequency)-resolved techniques, such as alternant current (AC) or impedance spectroscopy [18-21]. This work describes a comparative analysis of DC and AC response of the phthalocyanine based sandwich cells under steady-state action of water or mixed water/ammonia vapors.

## 2. Experimental details

The cells were fabricated by thermal evaporation of NiPc (from powder) on the standard glass/ITO substrates (ITO is double indium-tin oxide  $\text{In}_2\text{O}_3:\text{SnO}_2$ , surface resistance  $100 \Omega/\square$ ) purchased from Aldrich, followed by evaporation of

a top metal electrode, Al or In, through the shadow mask – Fig. 1. Active area of thus obtained cells, in both ITO/NiPc/Al and ITO/NiPc/In series, was  $10 \times 10 \text{ mm}$ . Thickness of NiPc layer was 50 nm in the ITO/NiPc/Al cells and 83 nm in the ITO/NiPc/In cells. An increased thickness of NiPc layer in the latter case is due to high risk of electrical shorts from top evaporated indium electrode down to the ITO substrate (Fig. 1), observed in our experiments. Thickness of metallic layer (Al or In) was 200 nm in all cases. More detailed description of the cell manufacturing process can be found in Refs. [17,19,20].

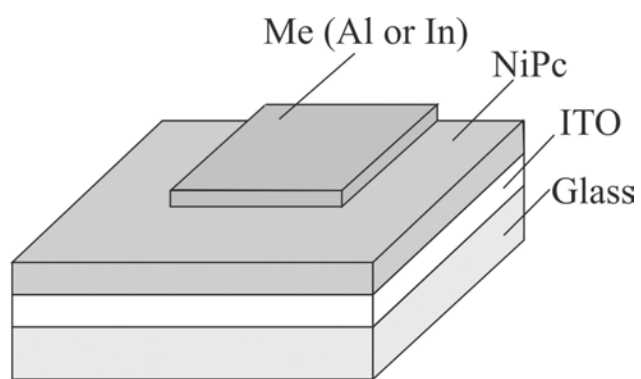


Fig.1. Schematic of the cells.

Immediately after fabrication, the cells were transferred to a measuring chamber. Electrical measurements were carried out in the dark, at room temperature, in the following atmospheres: dry air; saturated water vapor with pressure of 2.3 kPa; saturated mixed  $\text{H}_2\text{O}/\text{NH}_3$  vapors with partial pressures of 2.2/4.5 and 1.2/44.8 kPa. It is assumed that penetration of active molecules takes place through open surface of NiPc film between the contact strips.

DC conductivity measurements in the range of +2...-2 V were recorded using an AUTO-LAB measuring station (Eco Chemie) controlled by a General Purpose Electrochemical System (GPES) software. For  $J-V$  plots shown in Fig. 2,3, the sweeping rate was 0.025 V/s, with forward bias corresponding to a positively charged ITO electrode.

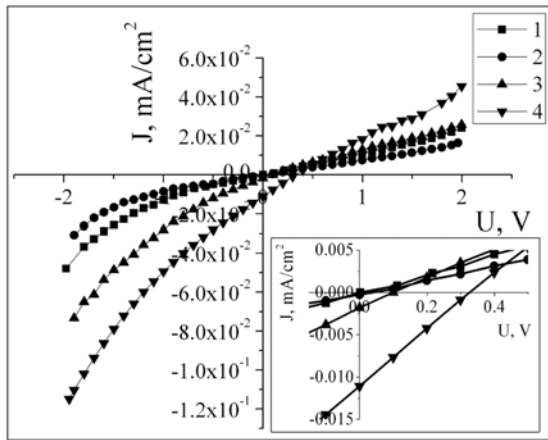
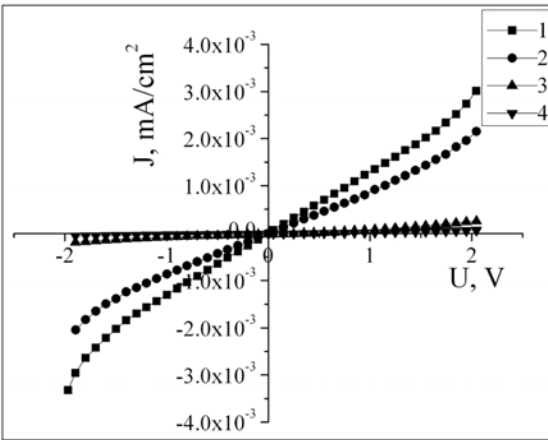
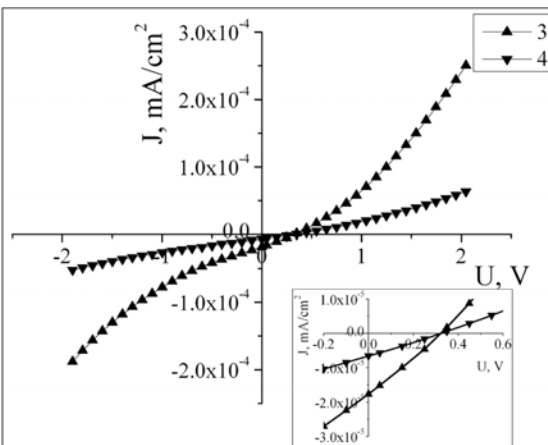


Fig. 2.  $J$ - $V$  plots for ITO/NiPc/Al cells in various atmospheres: 1- air; 2- saturated water vapor with pressure of 2.3 kPa; 3,4 - saturated ammonia vapor with partial  $\text{NH}_3$  pressure of 4.5 and 44.8 kPa (residual  $\text{H}_2\text{O}$  pressure 2.2 and 1.2 kPa, respectively).



(a)



(b)

Fig. 3.  $J$ - $V$  plots for ITO/NiPc/In cells in various atmospheres: 1- air; 2- saturated water vapor with pressure of 2.3 kPa; 3,4 - saturated ammonia vapor with partial  $\text{NH}_3$  pressure of 4.5 and 44.8 kPa (residual  $\text{H}_2\text{O}$  pressure 2.2 and 1.2 kPa, respectively).

Impedance spectra (AC conductivity) in the frequency range of  $10^{-2}$  to  $10^5$  Hz were obtained using AUTOLAB with Frequency Response Analyzer System (FRA-2) and GPES program, at constant bias of 1V. Then, the frequency dependences of impedance ( $Z$ ) were analyzed by graphic-analytical method using a ZView 2.3 (Scribner Associates) package. Relevancy of the derived models for experimental data was appropriate, as proved by a Kramers–Kronig coefficient that does not exceed  $3.10^{-5}$ . Inaccuracy of approximations for our models does not exceed 4%.

### 3. Results and discussion

#### 3.1. DC conductivity

##### 3.1.1. ITO/NiPc/Al cells

Experimental  $J$ - $V$  plots measured in the dark for the ITO/NiPc/Metal cells (where Metal=Al, In) in various atmospheres are shown in Fig. 2, 3. As seen from Fig. 2, the ITO/NiPc/Al cells do not practically show rectification in the given range of potentials in any environment, despite nominal work functions of top and bottom electrode materials are different [1-3]. Asymmetry of the electrodes manifests itself only in somewhat stronger non-linearity of  $J$ - $V$  plots under reverse bias.

The pure water vapor has little effect on the DC conductivity of ITO/NiPc/Al cells, which is different from the cells based on other phthalocyanines – cf. [12]. This would arise arises from differences in coordination activity of phthalocyanine complex with respect to small donor molecules [11] or in molecular packing. Nevertheless, the current density in humid air somewhat decreases, and  $J$ - $V$  curve is (very slightly) displaced from the point of origin – Fig. 2.

In mixed  $\text{H}_2\text{O}/\text{NH}_3$  vapors this displacement is much more pronounced and depends on ammonia content. Now, the 4<sup>th</sup> quadrant of the  $J$ - $V$  plot closely resembles typical plot of the illuminated cells (not shown) including bias polarity. Photovoltaic effect is not expected since the all measurements were done in the dark. Thus, the cells generate an output power  $P$  (similarly to [5,12,15]), its values are given in Table 1. As

Table 1.  
Parameters of dark DC plots

Parameter →	NH <sub>3</sub> Partial Pressure, kPa	$U_{oc}$ , V	$J_{sc}$ (mA/cm <sup>2</sup> )	$FF$	$P$ (mW)
<i>ITO/NiPc/Al</i>	4,5	0.1	0.002	0.2	0.004
	44,8	0.32	0.011	0.22	0.0078
<i>ITO/NiPc/In</i>	4,5	0.31	$1,8 \cdot 10^{-5}$	0.32	$0.18 \cdot 10^{-5}$
	44,8	0.31	$0,6 \cdot 10^{-5}$	0.27	$0.05 \cdot 10^{-5}$

seen from Table 1 and Fig. 2, the dark short circuit current  $J_{sc}^d$  increases concurrently with dark open circuit voltage  $U_{oc}^d$  as the ammonia partial pressure increases. In terms of photovoltaics, this would mean that both the film bulk and interfacial processes are important. It is worth mentioning that open circuit voltage and short circuit current appearing in these cells under illumination have even lesser magnitudes than those measured when the cells are exposed to H<sub>2</sub>O/NH<sub>3</sub> vapors in the dark (listed in Table 1). This also points to electrochemical nature of the generated power  $P$ .

### 3.1.2 ITO/NiPc/In cells

For the ITO/NiPc/In cells,  $J-V$  plots are weakly non-linear in dry air and humid environment – Fig. 3. Work function of indium is lower than that of aluminum (3.8 vs 4.3 eV). However, it does not form blocking contact to NiPc. According to Ref. [10], ohmic behavior of In contacts to phthalocyanines is not surprising, it originates from existence of thin (less than 1.5 nm) oxide layer. Work function of In<sub>2</sub>O<sub>3</sub> is comparable with work function of the second electrode ITO [22].

In wet atmosphere no displacement from the point of origin is observed. If ammonia is added, the dependences obey a power law  $J \sim U^n$ , where  $n$  varies from 1.53 to 1.75 depending on the pressure (Fig. 3b). This would imply a kind of space charge limited current (SCLC) [13]. Note, the current density decreases in presence of ammonia (Fig. 3a), contrary to the case of Al top electrode. Further decrease is observed with increasing pressure of ammonia vapors (Fig. 3b). Again, under these conditions both the dark short circuit current  $J_{sc}^d$  and the dark open circuit voltage  $U_{oc}^d$  are

clearly seen in the 4<sup>th</sup> quadrant of  $J-V$  plot – inset in Fig. 3b. Magnitude of  $J_{sc}^d$  is now much less than for the cells with aluminum top electrode, whereas the magnitudes of  $U_{oc}^d$  are comparable in these two cases. In the ITO/NiPc/In cells  $U_{oc}^d$  does not depend on ammonia pressure – Fig. 3 and Table 1.

## 3.2. AC conductivity

### 3.2.1. ITO/NiPc/Al cells

Fig. 4a, b shows Nyquist plots for ITO/NiPc/Al cells in dry air and in humid environment (H<sub>2</sub>O pressure of 2.3 kPa). Insets to Fig. 4a, b show corresponding equivalent circuits obtained using computerized parametric identification. In both cases they are composed of resistor  $R1$  and two  $R//C$  loops in series. Circuit parameters are given in Table 2. Here,  $CPE$  is a constant phase element. Generally,  $CPE$  represents formalism for description of the capacitance having a more complex physical nature. In our cells,  $CPE$  is just an elementary model that formally approximates some distribution of the object parameters and reflects destruction of interfacial capacitance by the corrosive processes [23]. Such equivalent circuit models are typical of the cells with phthalocyanine/metal interface [24]. Here,  $R1$  describes the value of contact resistance. The  $R3//C2$  element corresponds to the charge relaxation processes in the barrier area of the structure. With increasing frequency, the junction capacitance shunts the leakage of current through the barrier, thus the contribution of  $R3//C2$  element responsible for potential barrier can be neglected. At high frequencies, dominating role in the cell conductance turns to the  $R2//C1$  element, which

is responsible for hopping conductivity between localized states near the Fermi level in NiPc [19].

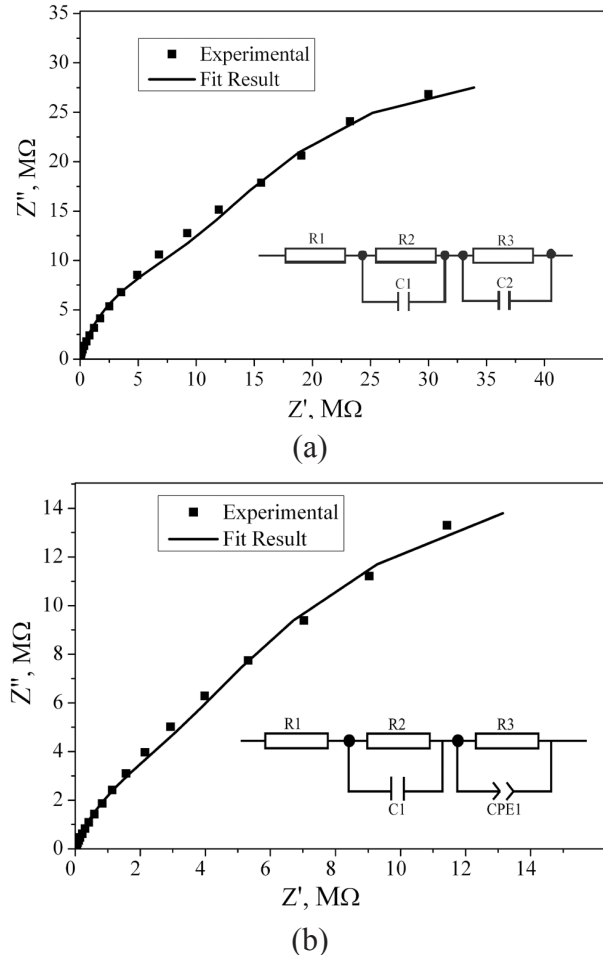


Fig. 4. Experimental Nyquist plots (symbols) and approximation results (lines) for ITO/NiPc/Al cells ((a)-air; (b)- 2.4 kPa  $\text{H}_2\text{O}$ ) with corresponding equivalent circuits in insets.

Introduction of ammonia vapors modifies the equivalent circuits for ITO/NiPc/Al cells, especially at low frequencies – Fig. 5. On the complex plane, this is better illustrated in Fig. 6, where experimental points in three different frequency ranges are compared in detail. In the high-frequency domain (1 MHz – 5 Hz), real part of the cell impedance ( $Z'$ ) becomes higher in all humid environments, as compared to dry air. The difference between dry and humid air decreases slightly at low frequencies (Fig. 6 a). For  $\text{NH}_3$ -containing environments there is an inversion point, at which the low-frequency impedance becomes lower (coming from high-frequency side), as shown in Fig. 6b, c. For the ammonia pressure of 4.5 Pa this change starts from 0.4 Hz, while for the pressure of 44.8 Pa it occurs at 5.2 Hz. Such a behavior suggests that the electrochemical component of

generated current is governed by some corrosion-like processes [16] that stimulate the rise of ionic component of conductivity at low frequencies.

Table 2.  
Calculated parameters of equivalent circuits shown in insets in Fig.4,5 and 7.

Atmosphere → Parameter ↓	1	2	3	4
in air	in $\text{H}_2\text{O}$ 2.3 kPa	in 4.5 kPa $\text{NH}_3$	in 44.8 kPa $\text{NH}_3$	
<i>ITO/NiPc/Al cells</i>				
$R1, \Omega$	255.8	285.2	243.5	253.3
$R2, \Omega$	$5.28 \cdot 10^7$	$4.3 \cdot 10^7$	$3.9 \cdot 10^6$	$6.05 \cdot 10^7$
$R3, \Omega$	$1.29 \cdot 10^7$	$9.02 \cdot 10^6$	-	-
$C1, \text{F}$	$3.63 \cdot 10^{-7}$	$6.44 \cdot 10^{-7}$	$1.4 \cdot 10^{-8}$	-
$C2, \text{F}$	$1.18 \cdot 10^{-7}$	-	-	-
$CPE, \text{F}$	-	$1.9 \cdot 10^{-7}$	-	$3.94 \cdot 10^{-7}$
$W, \text{Om} \cdot \text{cm}^2 \cdot \text{s}^{-1/2}$	-	-	32736	897.4
$\tau_1, \text{s}$	19.2	27.7	45.8	23.8
$\tau_2, \text{s}$	1.54	1.7	-	
<i>ITO/NiPc/In cells</i>				
$R1, \text{M}\Omega$	0.7	0.84	3.49	47.48
$R2, \text{M}\Omega$	1.6	3.27	16.6	417.2
$C1, \text{pF}$	2.54	2.05	2.13	2.97
$C2, \text{pF}$	0.086	-	-	-
$CPE, \text{nF}$	-	0.103	0.61	0.15
$\tau_1, \text{s}$	$1.8 \cdot 10^{-6}$	$1.71 \cdot 10^{-6}$	$5.3 \cdot 10^{-6}$	$1.4 \cdot 10^{-4}$
$\tau_2, \text{s}$	$1.4 \cdot 10^{-3}$	$2.4 \cdot 10^{-2}$	1.02	6.46

The increase of conductance through the cell in the low-frequency limit in presence of saturated  $\text{NH}_3/\text{H}_2\text{O}$  vapors correlates with DC conductivity measurements (Fig.2). Since free migration of small molecules and ions is possible inside of the thin NiPc layer, formation of alkaline condition in vicinity of top Al layer can be assumed when the cells are exposed to vapors by a well-known reaction:  $\text{NH}_3 + \text{H}_2\text{O} \rightarrow \text{NH}_4\text{OH}$ . Consequently, the highly dielectric  $\text{Al}_2\text{O}_3$  layer, which impedes injection and transport of charge carriers across the cell, will be etched off. At higher frequencies, the ionic component of current vanishes, and the effect of decreasing barrier area prevails.

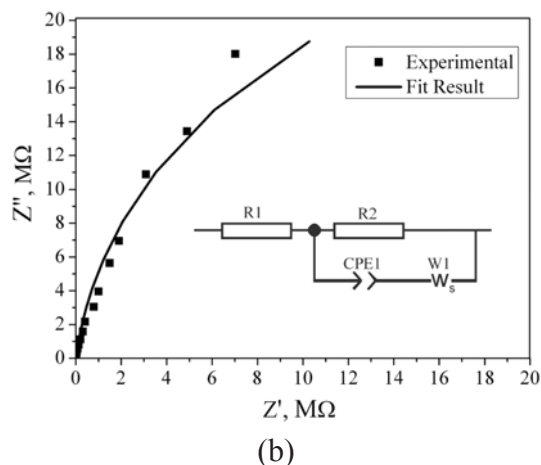
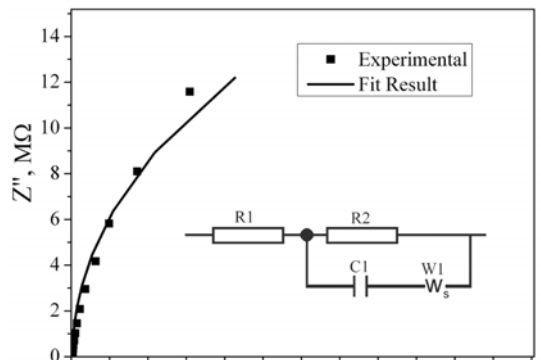


Fig. 5. Experimental Nyquist plots (symbols) and approximation results (lines) for the ITO/NiPc/Al cells ((a)- 4.5 kPa  $\text{NH}_3$ ; (b)- 44.8 kPa  $\text{NH}_3$ ) with corresponding equivalent circuits in insets.

To fit the Nyquist plots for ITO/NiPc/Al cells in the mixed water/ammonia vapors, equivalent circuits should be modified as shown in Fig. 5. As shown in Fig. 5a and 5b just one point in low frequency range of experimental results doesn't match with approximation curve, but average inaccuracy of modeling does not exceed 4%, giving background to conclude that the model is true. In these two cases, the electrochemical processes should be modeled by using diffusion impedance  $Z_w$  [23]. As follows from Table 2, value of Warburg coefficient  $W$  rapidly decreases with increasing  $\text{NH}_3$  vapor pressure. This is not surprising keeping in mind that Warburg coefficient is inversely proportional to the bulk concentration of diffusing species (assuming all other parameters, such as electrode area, diffusion coefficient, valency and temperature are constant). Therefore, reactions at the aluminum electrode are directly related to ammonia component in humid vapors.

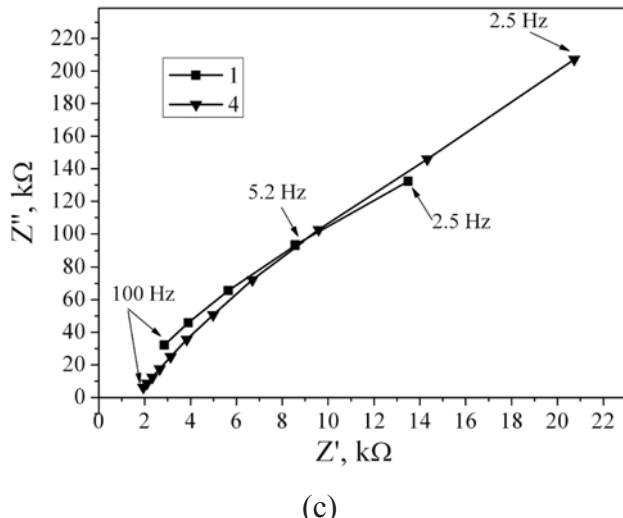
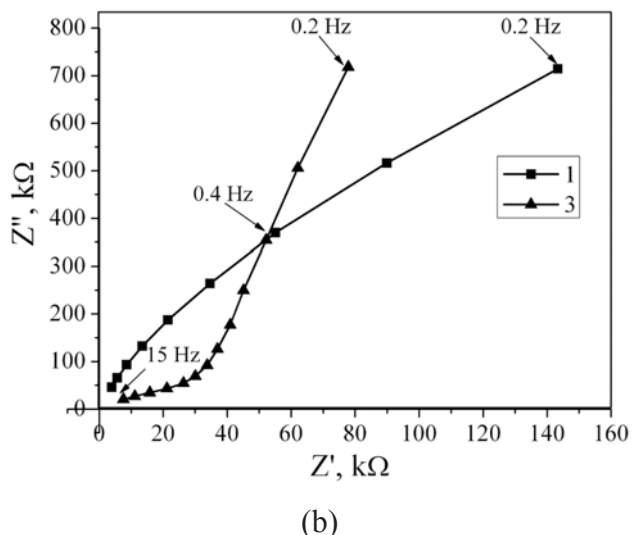
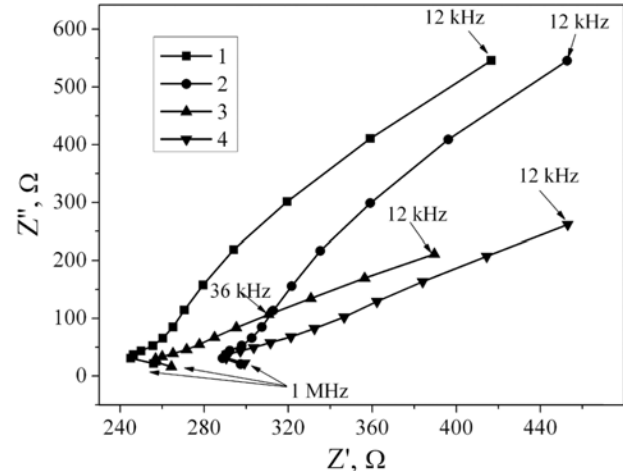
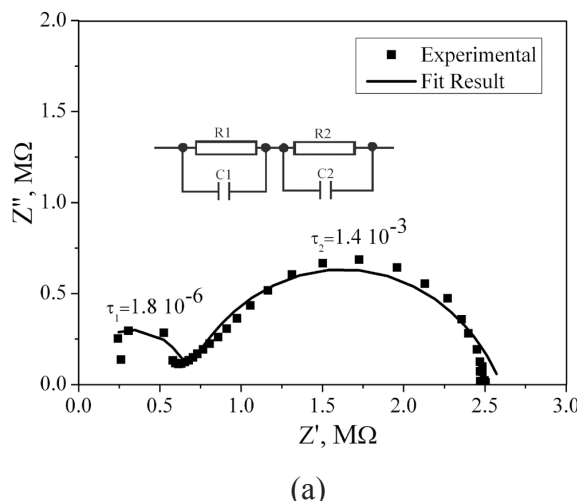


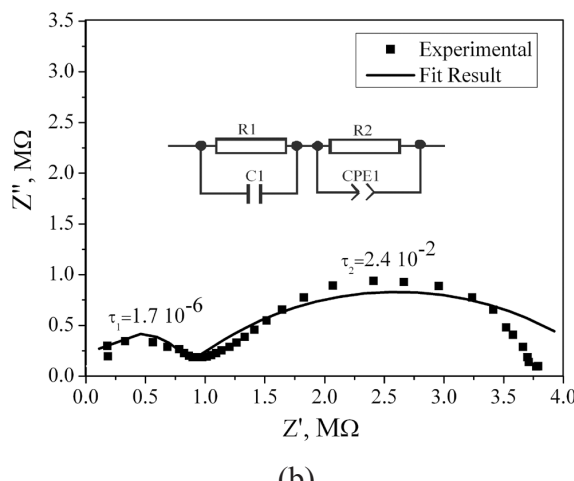
Fig. 6. Details of the complex plane (Nyquist plots) for ITO/NiPc/Al cells in different frequency ranges: (a) - 12 kHz–1 MHz, (b) – 0.2 Hz–15 Hz, (c) - 2.5 Hz–100 Hz. Conditions 1,2,3,4 as in Table 2.

### 3.2.2. ITO/NiPc/In cells

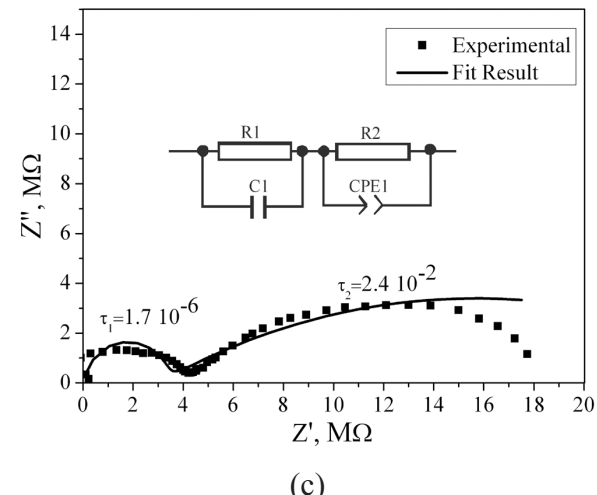
The Nyquist plots of ITO/NiPc/In cells in all environments are composed of two well-shaped semicircles [19,25] – Fig. 7a-d. Modeling of the impedance data gives equivalent circuits consisting of only two simple serial  $R//C$  elements (Fig. 7a-d, insets). The high-frequency  $R1//C1$  element characterizes the processes in the NiPc film bulk. It should be noted that relaxation times  $\tau_1$  ( $\tau_1=R1C1$ ) for ITO/NiPc/Al and ITO/NiPc/In cells differs very largely – Table 2. This might be ascribed to different thickness of NiPc layer in these cells (see, Experimental) and hence to its different morphology (e.g., orientation of molecules with respect to the substrate). Next, difference in relaxation times  $\tau_1$  and  $\tau_2$  observed for ITO/NiPc/Metal cells in every atmosphere is probably due to a higher degree of ordering in the film bulk [26] and to rather slow processes at disordered interfaces – Table 2.



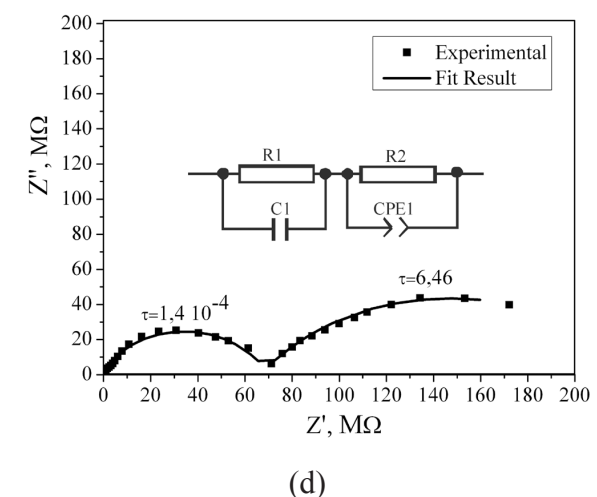
(a)



(b)



(c)



(d)

Fig. 7. Nyquist plots for ITO/NiPc/In cells (a) in air, (b) in water 2.3 kPa, (c) in ammonia 4.5 kPa, (d) in ammonia 44.8 kPa. Corresponding equivalent circuits are shown in insets, see Table 2 for parameters.

Equivalent circuit for ITO/NiPc/In remains unaltered when going from dry air to saturated  $\text{H}_2\text{O}$  or  $\text{NH}_3/\text{H}_2\text{O}$  vapors – Fig. 7a-d. Except the case of maximal  $\text{NH}_3$  pressure, the bulk relaxation time  $\tau_1$  (related to NiPc) does not markedly change – Table 2. Contrary to this, relaxation time  $\tau_2$  is largely affected by the humid environment and, especially, by ammonia vapor. For the ITO/NiPc/In cells, diffusion component of impedance was not revealed in presence of water and ammonia vapors, the shape of Nyquist plot is formed by the same two loops – Fig. 7c,d. This distinction with ITO/NiPc/Al cells can be caused e.g., by different position of metals in reactivity series (or in order of standard electrode potentials). Only the processes initiated at the top interface ‘NiPc/Met-

al' are considered, since here is a drop of potential and source of reactive sites (and ions). Redox processes at the second (bottom) interface 'ITO/NiPc' are less important, as follows from comparison of cells with different top electrodes.

As seen from Fig. 7c,d and Table 2, the overall resistance of ITO/NiPc/In cells increases with increasing NH<sub>3</sub> pressure. Similar effect was observed for series of metallophthalocyanines with the non-oxidized metallic contacts (Au, Cr, Pt) and studied as analytical response in chemical sensors in Refs. [9,13]. Several explanations can be proposed, taking into account coordination activity or energy levels of phthalocyanine complex. First is a compensation of resident molecular oxygen, almost unavoidable acceptor impurity that determines p-type semiconductivity of phthalocyanines [9,10], by absorbed ammonia molecules having unshared electronic pair (i.e., donor). Second explanation, from chemical viewpoint, would be displacement of oxygen molecule absorbed on the central metal atom of phthalocyanine complex by molecular ammonia, which has the same coordination position [11].

Existence of thin natural oxide layer on Al or In top electrode affects the conductivity of the NiPc based cells in different ways. In<sub>2</sub>O<sub>3</sub> layer is conductive [10], in contrast to insulating Al<sub>2</sub>O<sub>3</sub>, hence the dielectric barrier (interlayer) between metal and phthalocyanine layer is absent. Most probably, this determines a simplified equivalent circuit diagram for ITO/NiPc/In cells (insets in Fig. 4 and Fig. 7). Decrease of the cell conductivity is likely due to compensating effect of ammonia, as mentioned above. Conversely, in ITO/NiPc/Al<sub>2</sub>O<sub>3</sub>/Al cells an increase of conductivity occurs, as oxide dielectric interlayer is thinned (etched) by ammonium hydroxide. This is concurrent with the data shown in Table 2.

#### 4. Conclusion

DC conductivity measurements on NiPc based cells with Al or In top electrode exposed to different atmospheres (air, water and ammonia vapors) have shown that i) adding ammonia to water va-

pors leads to appearance of dark short circuit current  $J_{sc}^d$  and dark open circuit voltage  $U_{oc}^d$  in both types of cells; and ii) increase in partial vapor pressure of ammonia from 4.5 kPa to 44.8 kPa Pa leads to the increase of  $U_{oc}^d$  and  $J_{sc}^d$  for ITO/NiPc/Al cells in the range of 0.10–0.32 V and  $2 \times 10^{-3}$ – $1.1 \times 10^{-2}$  mA/cm<sup>2</sup>, respectively. For ITO/NiPc/In cells, change of  $J_{sc}^d$  in the range of  $1.8 \times 10^{-5}$ – $0.6 \times 10^{-5}$  mA/cm<sup>2</sup> is observed, whilst open circuit voltage remains unaltered with increasing vapor pressure ( $U_{oc}^d = 0.31$  V).

AC conductivity measurements on the ITO/NiPc/Al cells exposed to ammonia atmosphere reveal a more complex nature of charge transport. Under such conditions, both electronic and ionic current pathways may coexist. Modeling of AC response in the low-frequency domain (5 Hz–0.01 Hz) indicates ionic component of the current. It becomes more pronounced with increasing ammonia pressure, owing to electrochemical reactions at the NiPc/Al interface. Appearance of W in the equivalent circuit is caused by reactive sites on the top Al electrode, through which leakage of Faradaic current proceeds as soon as aluminum oxide is etched off in alkaline medium. The latter is formed after condensation of ammonia in wet atmosphere (i.e., NH<sub>4</sub>OH). The high-frequency domain (1 MHz–5 Hz) is dominated by electronic component of conductivity. It is associated with the hopping transport of charge carriers between localized states near the Fermi level of NiPc.

The cells with In electrode do not practically show the diffusion component of current when exposed to ammonia, which is in contrast with the ITO/NiPc/Al cells. The shape of impedance curves is formed by two semicircles and undergoes only quantitative changes with increasing ammonia pressure. The equivalent circuit for the ITO/NiPc/In cells consists of two serial  $R//C$  elements in any environment. Relaxation time  $\tau_1$ , corresponding to the first  $R1//C1$  element responsible for the film bulk, changes moderately (in the range of  $\mu$ s). For the interfacial area, which is assigned to the second  $R2//C2$  element, relaxation time  $\tau_2$  varies from  $1.4 \cdot 10^{-3}$  to 6.46 s with changing environment.

## References

1. C.Y. Kwong, Djurisic, P.C. Chui, S.M. Lam, W.K. Chan, Improvement of the efficiency of phthalocyanine organic Schottky solar cells with ITO electrode treatment // *Appl. Phys.* – 2003. - A 77. – P. 555-560.
2. K. Takahashi, T. Gosa, T. Yamaguchi, T. Komura, K. Murata, Enhanced Photocurrent in Al/Porphyrin Schottky Barrier Cell with Heterodimer Consisting of Metal-Free Porphyrin and Zinc Porphyrin // *J. Phys. Chem.* – 1999. - B 103. – P.4868-4875.
3. M. Shah, M.H. Sayyad, Kh.S.Karimor, M.Marоof-Tahir, Investigation of the electrical properties of a surface-type Al/NiPc/Ag Schottky diode using I-V and C-V characteristics // *Physica*. – 2010. B 405. – P.1188-1192.
4. V. Singh, S. Rajaputra, G. Chintakula, G. Sagi, S. Phok, Schottky diode solar cells based on copper phthalocyanine nanowires // IEEE Conference Publications, 33rd IEEE Photovoltaic Specialists Conference, San Diego, CA, USA. – 2008. P.1-6.
5. K. Shinbo, M. Minagawa, H. Takasaka, K. Kato, F. Kaneko, T. Kawakami, Electrical and luminescent properties due to gas adsorption in electroluminescent device of metal-free phthalocyanine // *Colloids Surf.* - A 198/200. – P.905-909.
6. I. Muzikante, V. Parra, R. Dobulans, E. Fonavs, J. Latvels, M. Bouvet, A Novel Gas Sensor Transducer Based on Phthalocyanine Heterojunction Devices // *Sensors*. – 2007. - 7/11. – 2984-2996.
7. H.R. Kerp, K.T. Westerduin, A.T. van Veen, E.E. van Faassen, Quantification and effects of molecular oxygen and water in zinc phthalocyanine layers // *J. Mater. Res.* – 2001. – 16. – P.503-511.
8. A. Belghachi, R. A. Collins, The effects of humidity on phthalocyanine NO<sub>2</sub>, and NH<sub>3</sub>, sensors // *J. Phys. D Appl. Phys.* – 1990. – 23. – P.223-227.
9. H. Tachikawa and L. R. Faulkner, Electrochemical and Solid State Studies of Phthalocyanine Thin Film Electrodes // *J. Am. Chem. Soc.* – 1978. - 1 100/14. – P.4379.
10. A.K. Hassan and R.D. Gould, The electrical properties of copper phthalocyanine thin films using indium electrodes // *J. Phys. D Appl. Phys.* – 1989. – 22. – P.1162.
11. A.A. Ovchinnikov, G.L. Pakhomov, V.N. Spector, Mass effect under ammonia sorption by copper simmdichlorophthalocyanine films // *Reports of the Russian Academy of Sciences*. – 1994. - 338/4-6. – P.18.
12. G.L. Pakhomov, L.G. Pakhomov, V.V. Travkin, M.V. Abanin, P.Y. Stakhira, V.V. Cherpak, Phthalocyanine-based photoelectrical cells: effect of environment on power conversion efficiency // *J. Mater. Sci.* – 2010. – 45. – P.1854-1858.
13. A. Miller, R.D. Yang, M.J. Hale, J. Park, B. Fruhberger, C.N. Colesniuk, I.K. Schuller, A.C. Kummel, W.C. Troglar, Electrode Independent chemoresistive response for cobalt phtalocyanine in the space charge limited conductivity regime // *J. Phys. Chem. B*. – 2006. – 110. – P.361-366.
14. T.-H. Lee, J.-C. Huang, G.L. Pakhomov, T.-F. Guo, T.-C. Wen, Y.-S. Huang, C.-C. Tsou, C.T. Chung, Y.-C. Lin, Y.-J. Hsu, Organic-Oxide Cathode Buffer Layer in Fabricating High-Performance Polymer Light-Emitting Diodes // *Adv. Funct. Mater.* – 2008. – 18. – P.1-7.
15. G.L. Pakhomov, V.V. Travkin, P.Y. Stakhira, V.V. Cherpak, D. Volyniuk, Electrical properties of phthalocyanine-based sandwich cells with embedded ultrathin metallic layer // *Mol. Cryst. Liq. Cryst.* – 2011. – 5350. – P.42-48.
16. K. Murata, S. Ito, K. Takahashi, B. M. Hoffman, Photocurrent from photocorrosion of aluminum electrode in por-

- phyrin/Al Schottky-barrier cells // Appl. Phys. Lett. – 1997. – 71. – P.674-676.
17. V. Cherpak, P.Y. Stakhira, O.I. Kuntyy, A. Zakutayev, Study of Barrier Structures on the Base of Nickel Phthalocyanine Thin Films During the Interaction with the Ammonia Medium // Mol. Cryst. Liq. Cryst. – 2008. – 496. – P.131-137.
18. W. Riess, S. Karg, V. Dyakonov, M. Meier, and M. Schwoerer, Electroluminescence and photovoltaic effect in PPV Schottky diodes // Journal of Luminescence. – 1994. – 60/61. – P.906-911.
19. P.Y. Stakhira, I.I. Grygorchak, V.V. Cherpak, F.O. Ivastchyn, D.Y. Volynyuk, G. Luka, M. Godlewski, E. Guziewicz, G.L. Pakhomov, Z.Y. Hotra, Long time stability of ITO/NiPc/ZnO/Al devices with ZnO buffer layer formed by atomic layer deposition technique - impedance spectroscopy analysis // Mater. Sci. Eng. – 2010. - B 172. – P.272-275.
20. P.Y. Stakhira, G.L. Pakhomov, V.V. Cherpak, D. Volynyuk, G. Luka, M. Godlewski, E. Guziewicz, Z. Yu. Hotra, Photovoltaic cells based on nickel phthalocyanine and zinc oxide formed by atomic layer deposition // Cent. Eur. J. Phys.. – 2010. – 8. – P.798-803.
21. Y. Liu, A. Liu, Z. Hu, W. Liu, F. Qiao, Impedance spectroscopy studies on CuPc/n-Si hybrid solar cell // J. Phys. Chem. Solids. – 2012. – 73. – P.626-629.
22. J. Olivier, B. Servet, M. Vergnolle, M. Mosca, G. Garry, Stability/Instability of Conductivity and Work Function Changes of ITO Thin Films, UV-Irradiated in Air or Vacuum. Measurements by the Four-Probe Method and by Kelvin Force Microscopy // Synth. Met. – 2001. – 122. – P.87-89.
23. E. Arsoukov, J. Ross Macdonald, Impedance Spectroscopy. Theory, Experiment and Applications // New-York NY. – 2005. - P.606.
24. G. L. Pakhomov, V. I. Shashkin, D. E. Pozdnyayev, C. Muller, J. M. Ribo, AC measurements on binary phthalocyanine films // Org. Electron. – 2002. - 3/3-4. – P.93-103.
25. S. Karg, M. Meier, and W. Riess, Light-emitting diodes based on poly-p-phenylene-vinylene: I. Charge-carrier injection and transport // J. Appl. Phys. – 1997. – 82. – P.1951-1960.
26. V.S. Reddy, S. Das, S. K. Ray, A. Dhar, Studies on conduction mechanisms of pentacene based diodes using impedance spectroscopy // J. Phys. D Appl. Phys. – 2007. – 40. – P.7687-7693.